PIBBS
PROGRAM IN INTERDISCIPLINARY BIOLOGICAL & BIOMEDICAL SCIENCES

Sandia National Laboratories
SAND2010-1390C

Distribution and dynamics of RBL IgE receptors (FcεRI) observed quantitatively on planar ligand-presenting surfaces

Kathrin Spendier†, Amanda Carroll-Portillo‡, Keith Lidke§, Bridget S Wilson‡, Jerilyn A. Timlin¶, V. M. Kenkre† and James L. Thomas§

†Consortium of the Americas for Interdisciplinary Science, and Department of Physics and Astronomy, University of New Mexico, Albuquerque, New Mexico 87131, USA
‡Departments of Pathology and §Physics and Astronomy, University of New Mexico, Albuquerque, New Mexico 87131, USA
¶Sandia National Laboratories, Albuquerque, New Mexico 87185-0895

THE UNIVERSITY of NEW MEXICO

UNIVERSITY of NEW MEXICO CANCER CENTER

Consortium of the Americas for Interdisciplinary Science

ABSTRACT

There is considerable interest in the signaling mechanisms of immunoreceptors, especially when triggered with membrane-bound ligands. When T cells, B cells, or mast cells bind to monovalent ligands on fluid supported lipid bilayers, receptor clustering, signaling, and receptor redistribution into immunological synapses follow. We have quantitatively studied the kinetics of redistribution of IgE receptors (FcεRI) on RBL-2H3 mast cell surfaces. To separate the kinetics of receptor redistribution from cell spreading, the initial cell-substrate contact time was precisely defined (±50 ms) by micropipet cell manipulation. Using total internal reflection fluorescence, the distribution and dynamics of receptor clusters were imaged. We find strong quantitative evidence that initial receptor aggregation occurs at cellular protrusions, which are visible bright spots/regions on cells contacting ligand-free surfaces. The initial size of these regions is independent of the substrate and the presence or absence of ligand, and they were found to be randomly distributed over the interfacial contact area. Using a finite-element diffusion model, we found that the initial rate of accumulation of receptors at the protrusions is consistent with diffusion-limited trapping with D ~10^{-1} μm²/s. At longer timescales, individual clusters on ligand-bearing membranes were observed to move with both a diffusive and a directed component of motion; after an initial delay clusters eventually coalesced near the center of the contact region (~ 1 minute).

INTRODUCTION

The goal is to investigate dynamics and organization of mast cell surface receptors through experimental and theoretical studies after the initial contact with monovalent ligands in supported fluid bilayers. It is known that monvalent ligands in fluid membranes can trigger mast cells through the formation of IgE receptor microclusters (Weis 1982). Weis at al. have suggested that the mechanism by which laterally mobile haptens could aggregate IgE receptors is driven by cell surface roughness, via receptor diffusion to points of close contact. Here we present the first quantitative measurement which confirms this well accepted hypothesis (Metzger 1992). In our recent work we also showed, for the first time, that receptor clusters coalesce within a few minutes to form a large central patch termed mast cell synapse (Carroll-Portillo 2010). Whereas the formation kinetics of the immunological synapse in T cells has been modeled nothing is known about the kinetics which drive the mast cell synapse formation. To describe these kinetics we develop a new theory of aggregation which generalizes Smoluchowski's (Chandrasekhar 1943) well known theory for arbitrary melding probability.

Experimental Methods: Initial contact time is determined to within 50 ms.

Total internal reflection (TIRF) microscope was used to visualize fluorescently labeled (Alexa488 or DY520-XL) IgE-loaded receptors on RBL-2H3 cells.

First cell contact with a ligand-presenting surface was fixed within ~50 ms by a micropipette manipulation technique (Waugh 1979).

The ligands presented were:

(1) mobile in supported fluid lipid bilayer; POPC bilayers were made with monovalent ligand DPPE-caproyl-DNP (Avanti Polar Lipids) at 0, 1, 5, 10, and 25 mol%.

(2) immobile in supported lipid bilayer; DPPC bilayer was made with monovalent ligand DPPE-caproyl-DNP at 25 mol%.

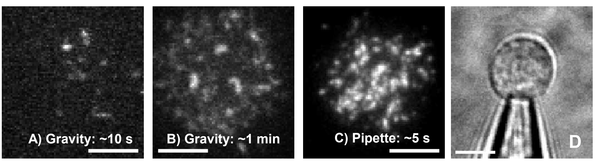

FIGURE 1 (A, B) TIRF images of DY520-XL-labeled IgE in receptor clusters, on a RBL-2H3 cell in contact after approximately (A) ~10 s and (B) ~1 min with a POPC bilayer with 10 mol% ligand lipids. Cell settled due to gravity. (C) TIRF image of Alexa488-labeled IgE on a RBL-2H3 cell at initial contact (~5 s) with a POPC bilayer with 25 mol% ligand lipids. This cell was pushed down with a micropipette. (D) a micrograph showing a RBL-2H3 cell held approximately 1 μm above the surface with a micropipette. Bar = 5 μm.

Explicit noise removal applied to Image Correlation Spectroscopy

Image correlation spectroscopy (ICS) was used to quantitatively measure receptor distributions on cell surfaces (Petersen 1993). ICS involves computing the two dimensional spatial autocorrelation function, $g(\varepsilon,\eta)$ of an image $i(x,y)$:

Eq.1 $$g(\varepsilon,\eta) = \frac{\langle i(x,y)i(x+\varepsilon,y+\eta)\rangle}{\langle i\rangle^2} - 1.$$

In systems without orientational order, all the information in the correlation function is contained in its rotational average, $g(r)$ and the width of this distribution is a measure of the spatial scale of heterogeneities. The variance of the fluctuations includes a dominant contribution from uncorrelated noise from camera read noise, σ_r, and shot noise, σ_p. The noise corrected rotationally averaged correlation $g(0)_{corr}$ can be obtained by (Unruh 2008):

Eq.2 $$g_{corr}(0) = g(0)_{raw} - \frac{\langle \sigma_r^2 + \sigma_p^2 \rangle}{\langle i\rangle^2}.$$

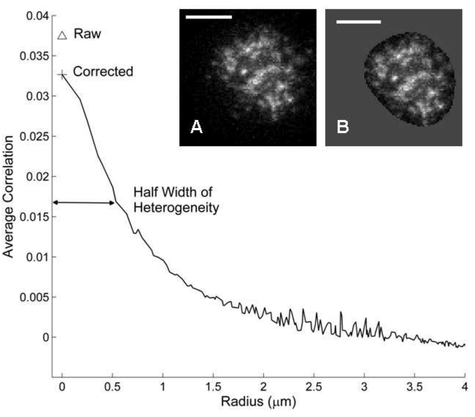

Figure 2 Image correlation was performed to determine the size of heterogeneity and g(0) of single cells pipette-pressed against a stimulating surface. Rotationally averaged correlation showing explicit noise removal (Spendier et al. submitted) and half width of receptor clusters. (A) TIRF image of pipette-pressed RBL-2H3 cell loaded with 488Alexa-IgE on a bilayer with 1 mol% DNP-lipid. (B) Image masked with mean of cell interior. Bar = 5μm.

The mechanism of IgE receptor aggregatation is trapping at cell protrusions.

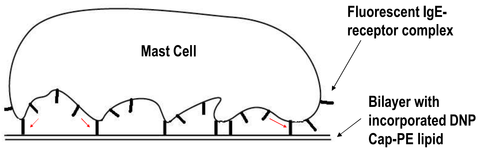

Figure 3 After initial contact with a ligand presenting surface, contact points brighten due to diffusion of unbound IgE-receptor complexes to the contact points.

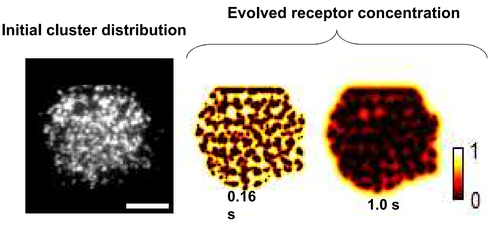

Figure 4 To test this mechanism, initial contact zones were taken as traps in a 2D finite element diffusion model in Matlab. Bar = 5 μm.

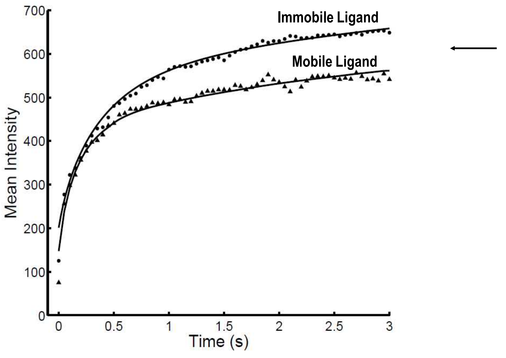

Figure 5 Mean receptor cluster intensity is used as a measure of number of receptors trapped in cell protrusions over time due to (DPPC) immobile and (POPC) mobile ligands in bilayer. The data was fit to a numerical 2D diffusion model, in which receptors get trapped in cell protrusions. The numerical model was fit up to 3 s and for both surfaces the model fit the data well. The mean diffusion coefficients were 0.30 ± 0.08 μm²/s and 0.24 ± 0.07 μm²/s for DPPC and POPC respectively. The error represents the standard error of the mean of at least three measurements. The extracted diffusion coefficients for data presented here were 0.16 μm²/s and 0.26 μm²/s for DPPC and POPC respectively (Spendier et al. submitted).

IgE receptor clusters are randomly distributed and undergo a combination of diffusive and directed motion.

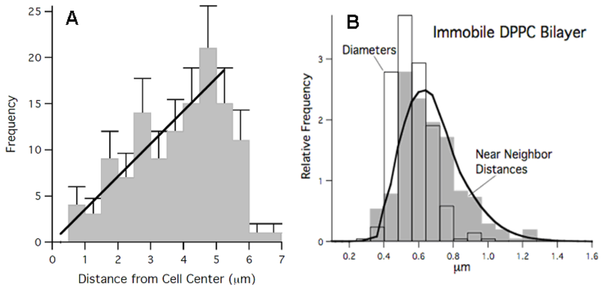

Figure 6 (A) The number of cluster at a radial distance r is proportional to the distance from the center of a cell (Fig. 5A) as expected for a uniform density of randomly positioned clusters. (B) Distribution of cluster diameters and nearest-neighbor distances on immobile ligand substrates. The area of each bar is the fraction of clusters with nearest-neighbor distances (grey bars) or diameters (white bars) in the x-range of the bar. The solid lines are the nearest-neighbor distances expected from a random spot model, weighted with the measured distribution of cluster diameters (Spendier et al. submitted).

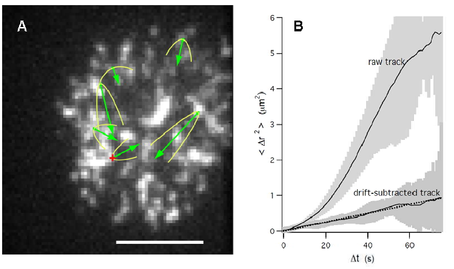

Figure 7 (A) Tracked IgE receptor clusters after about 55 s of initial contact on POPC bilayer with 25 mole % DNP lipid. Yellow parabolas show the cluster's root mean squared diffusional spread. Green arrows are proportional to the drift velocity and show how far each cluster would drift in 66 s. Bar = 5 μm. (B) Raw and drift-subtracted mean squared displacement for cluster track indicated with red **+** in (A). Shaded area represents the standard error of the mean from multiple measurements. The mean diffusion coefficient and flow speed from multiple measurements were 5.1 ± 0.7 · 10⁻³ μm²/s and 37 ± 5 nm/s respectively (Spendier et a. submitted).

Receptor clusters coalesce to form a mast cell synapse and a depletion zone.

On mobile ligands within minutes, receptors on pipette-pressed and settling cells formed a large centralized region of receptors, called the mast cell synapse (Carroll-Portillo 2010). This central region of clusters was not observed on immobile surfaces (data not shown). Figure 8 depicts the maturation of the mast cell synapse over time. The rotationally averaged correlation function contains spatial information of receptor clusters and suggests that mast cell synapse maturation is represented by a radial anti-correlation in g(r). This anti-correlation seems to be consistent with the appearance of a receptor depletion zone.

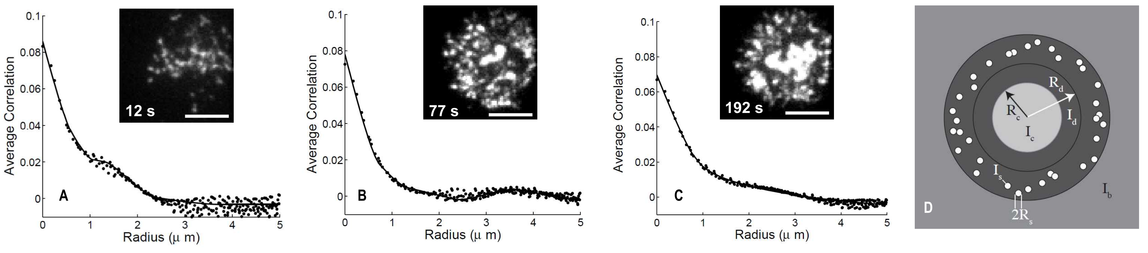

Figure 8 (A), (B), and (C) depict rotationally averaged correlation of a RBL cell pipette-pressed on POPC bilayer with 25 mole % DNP lipid fit to a six parameter receptor depletion model (D) for three different time intervals: (A) 10 to 14 s, (B) 75 to 79 s, and (C) 190 to 194 s. Images were taken every second and each correlation plot represents the mean of five successive rotationally averaged correlation functions. The six parameter model fits the data rather well and estimates the radius of small and central cluster for different time intervals after initial contact. (E) Model extracted small and central cluster radii over time. Arrows indicate data depicted in (A), (B), and (C). Missing data points indicate that depletion model could not be fit.

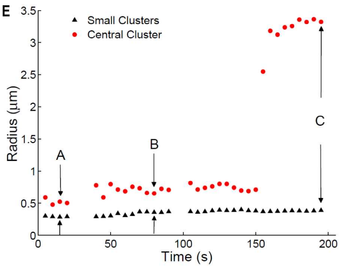

General development when melding process is not instantaneous.

Figure 8 Schematic illustration of a piece of the 1-d lattice with periodically placed links of transfer rate F. The random walker starts initially at site m=0 and eventually gets trapped at site m=r at a finite rate C.

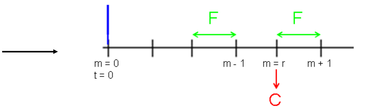

Eq.3 $$\frac{dP_m}{dt} = F\left(P_{m+1} + P_{m-1} - 2P_m\right) - \delta_{m,r} C P_m$$

$$\tilde{P}_m(\varepsilon) = \tilde{\eta}_m(\varepsilon) - C\frac{\tilde{\Psi}_{m-r}(\varepsilon)\,\tilde{\eta}_r(\varepsilon)}{1 + C\tilde{\Psi}_0(\varepsilon)}$$

$$\tilde{Q}(\varepsilon) = \sum_m \tilde{P}_m(\varepsilon) \longrightarrow \frac{dQ(t)}{dt} = -k(t)\,Q(t)$$

To gain physical insight we analyze a discrete Master equation (e.g. translatioanlly invariant hopping rate, Eq.3) on a 1-d lattice and solve the problem to quadratures via the defect technique and then take the continuum limit.

$\tilde{}$ denotes the Laplace transform and ϵ the Laplace variable
$P_m(t)$: Probability to be at site m
$\eta_m(t)$: Solution of Eq.3 in the absence of a absorber
$\Psi_{m-r}(t)$: Probability of finding particle at site m if it started at site r
$Q(t)$: Probability to find particle anywhere
$k(t)$: 1-d genreal transition rate for stationary absorber problem

In 1-d continuous space, the exact solution for the perfect absorber problem (C=∞) for a particle initially placed at x_0 is given in Eq.4 (Spouge 1988, Doering 1989). The equivalent imperfect absorber problem has been solved by Abramson and Wio (1996) which we derived independently, Eq.5. Here we note that the total probability Q(t) in Eq.5 has two features in the physical limits: times add (Kenkre and Wong, 1981) ; and probabilities multiply (Kashchiev 2000).

Eq.4 $$Q(t, x_0) = erf\left(\frac{x_0}{\sqrt{4Dt}}\right)$$

$\tau = \frac{x_0^2}{D}$: Time it takes to reach absorber
$\zeta = \frac{2D}{\mathcal{C}x_0}$: Describes the absorption process
D: Diffusion constant in m^2/s
$\mathcal{C}$: Capture speed in m/s

Eq.5 $$Q(t, x_0) = erf\left(\frac{1}{2}\sqrt{\frac{\tau}{t}}\right) + e^{\frac{1}{\zeta}+\frac{1}{\zeta^2}\left(\frac{t}{\tau}\right)} erfc\left(\frac{1}{2}\sqrt{\frac{\tau}{t}} + \frac{1}{\zeta}\sqrt{\frac{t}{\tau}}\right)$$

Eq.6 $$\frac{dP_m(t)}{dt} = \text{motion terms} - c\sum_r{}' \delta_{m,r} P_m(t)$$

Eq.7 $$\frac{dQ(t)}{dt} = -\int_0^t dt' \mathcal{M}(t-t')\underbrace{\left(\sum_r{}' P_r(t')\right)_0}$$

Homogeneous solution at absorber site in absence of absorber

Eq.8 $$\tilde{\mathcal{M}}(\epsilon) = \frac{1}{\frac{1}{c} + \tilde{\nu}(\epsilon)}$$

For a particle occupying a site m in discrete space of arbitrary dimensions with probability $P_m(t)$ at time t, which moves in some fashion (with or without coherence, with or without translational invariace, etc.), the Master equation is given in Eq.6. One can solve Eq.6 via the defect technique and obtain the rate of change of the total probability, Eq.7. The important quantity in Eq.7 is the memory term $\mathcal{M}(t)$ which is precisely given by Eq.8. The memory term is determined by the motion parameters and the ν-function. The idea of the ν-function was put forward in 1982 by Kenkre. It is the sum of propagators of the homogeneous system (in the absence of traps) from one trap location to all others.

New Aggregation Theory

The total probability Q(R,t) decreases by a certain explicitly known rate h(R,t) which depends on the size R of the absorber, Eq.9. This rate is also the rate at which R increases, Eq.10 (e.g. in 1-d). Combining Eq.9 and Eq.10 leads to Eq.11 that can be solved for R(t). Finally, solving Eq.11 and Eq.9 simultaneously produces a completely new aggregation theory.

Eq.9 $$\frac{dQ(R,t)}{dt} = h(R,t)$$

Eq.10 $$\frac{dR(t)}{dt} = -const \cdot h(R,t)$$

$\tau = \frac{x_0^2}{D}$: Time it takes to reach absorber
$\zeta = \frac{2D}{\mathcal{C}x_0}$: Describes the absorption process
D: Diffusion constant in m^2/s
$\mathcal{C}$: Capture speed in m/s

Eq.11 $$Q(R(t),t) - Q(R(t),t) = const \cdot [R(0) - R(t)]$$

Eq.12 $$Q(R(t),t) = erf\left(\frac{1}{2}\sqrt{\frac{\tau}{t}}\left(1 - \frac{R_0}{x_0} - \frac{R(t)}{x_0}\right)\right) + e^{\frac{1}{\zeta}\left(1-\frac{R_0}{x_0}-\frac{R(t)}{x_0}\right)+\frac{1}{\zeta^2}\frac{t}{\tau}} erfc\left(\frac{1}{2}\sqrt{\frac{\tau}{t}}\left(1 - \frac{R_0}{x_0} - \frac{R(t)}{x_0}\right) + \frac{1}{\zeta}\sqrt{\frac{t}{\tau}}\right)$$

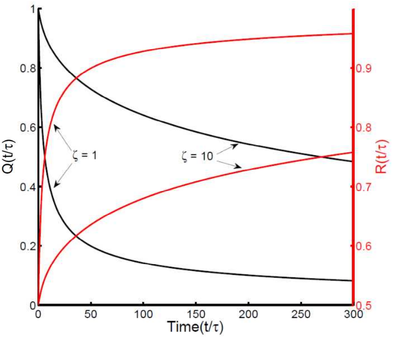

Figure 9 Time evolution of total probability Q(t) and stationary absorber radius R(t) for a rod of diameter $2R_0$ initially placed at x_0 given in Eq. 12. As the melding probability increases, the absorber radius reaches its final value more rapidly. Here we note that the radius increases exponentially.

Aggregation theory applied to experiment: Receptor cluster coalescence is ~40s delayed.

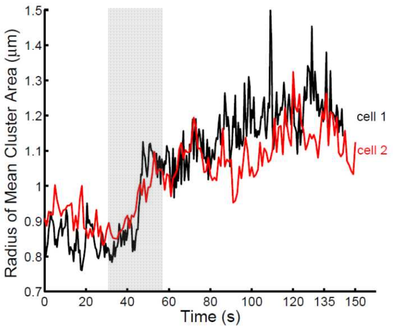

Figure 10 Measured radius of mean cluster area over time follows a s-shaped curve. This quantitative measurement with qualitative observations that only at late time points (>1min) every contact of two clusters leads to melding, supports the contention that receptor cluster coalescence is delayed. Theoretically, if cluster coalescence were not delayed, the absorber radius would increase exponentially (Fig. 9).
The delay in coalescence might be due to actin reorganization. At early time points receptor cluster interactions with the actin cytoskeleton restrict cluster coalescence (Kaizuka 2007), while at late time points the formation of an actin-poor central mast cell synapse (Carroll-Portillo 2010) makes cluster melding more probable. Here, two cells were pipet pressed on POPC bilayer with 25 mole % DNP lipid. At each time step the average cluster area was computed from which the reported radius was determined. The grey rectangle highlights a time interval during which the melding process becomes more probable.

CONCLUSIONS

- **The mechanism of receptor clustering is trapping at cell protrusions.**
- **Receptor clusters that are initially randomly distributed, move with both diffusive and directed motion components and eventually coalesce to form a mast cell synapse that is accompanied by a receptor depletion zone.**
- **We developed a new generalized aggregation theory which hold foe arbitrary melding probability, dimensions, and motion.**
- **Experimental data applied to general aggregation theory suggests that receptor cluster coalescence is delayed by ~40 s.**

Abramson and Wio, 1996, *Phys. Rev. E.*, 53: 2265-2270
Carroll-Portillo, et al. 2010. *J. Immunol.* 184: 1328-1338
Chandrasekhar, S., 1943. *RMP* 15: 1-89
Doering and ben-Avraham, 1988, *Phys. Rev. A* 38: 3035-3042
Kaizuka, Y., et al. 2007. *PNAS*. 104: 20296-20301
Kashchiev, 2000, Nucleation: Basic Theory with Application
Kenkre, 1982, *Chem. Phys. Lett.* 93: 260
Kenkre and Wong, 1981, *Phys. Rev. B* 23: 3648
Metzger, H., 1992. *J. Immunol.* 149(5):1477-87.
Petersen, N. O., et al. 1993. *Biophys.* 65: 1135-1146
Spendier K. et al., submitted. *Biophys. J.*
Spouge, 1988, *Phys. Rev. Let.* 60: 871-874
Unruh, J. R. and E. Gratton. 2008. *Biophys. J.* 95: 5385-5398
Waugh, R. and E. A. Evans. 1979. *Biophys. J.* 26:115.
Weis, R. M., et al. 1982. *Biological Chemistry* 257(11):6440-5.

Sandia is a multi-program laboratory operated by Sandia Corporation, a Lockheed Martin Company, for the United States Department of Energy under Contract DE-ACO4-94AL85000. Kathrin Spendier is supported by the Program in Interdisciplinary Biological and Biomedical Sciences funded by the University of New Mexico and by the ARO grant (W911NF-05-1-0464). The authors would like to express their gratitude and thanks towards Dr. Fernando C. Valenzuela for helping me with pulling micropipettes and the technicians in Dr. Bridget S. Wilson's lab.